Vegetation Dynamics and Their Contribution to the Little Ice Age

Nabil Swedan[1*]
[1]Pacific Engineering PLLC, Redmond, WA, U.S.A.

*Correspondence to: Nabil Swedan
9350 Red-Wood Rd. NE, B210
Redmond, Washington, 98052, U.S.A.
nabilswedan@yahoo.com
swedan@pacificengineeringpllc.com
https://orcid.org/0000-0003-1976-5516

The paper is a non-peer reviewed preprint submitted to EarthArXiv. However, the preprint was submitted to a journal for peer review.

Abstract

Causes of the Little Ice Age (LIA) have remained a subject of intensive research due to its significance. The causes of the LIA have been largely speculative; however, recent studies suggest that plant and vegetation growth may provide a plausible explanation. The LIA period coincided with an ecological encounter, as humans from the Old and New Worlds exchanged goods and diseases. A significant portion of the global population was decimated, leading to the abandonment of farmlands, which nature subsequently reclaimed. This shift in vegetation dynamics and interaction with their environment is analyzed. One example is the thermodynamic cycle of aquatic photosynthesis, which requires a flow of seawater as a medium for heat transfer. The flow interacts with ocean currents that connect the deep ocean to surface waters. As plants and vegetation grow, cold deep-ocean water is brought to the surface, leading to a decrease in surface temperature. This cooling effect is time-dependent: the longer the vegetation grows, the cooler the surface becomes. Even small amounts of vegetation growth over extended periods could trigger glaciations. Such ice ages can be devastating for global ecosystems, and their future occurrence remains a possibility. Therefore, climate management should be a priority for human society.

Keywords: Little Ice Age; Photosynthesis; Carnot Cycle; Air Psychrometry; Thermohaline Circulation; Theoretical Model

1. Introduction

The Little Ice Age (LIA) is characterized by a relevant cooling of the Earth's surface temperature that occurred before 1850, prior to the instrument records. The LIA, therefore, offers a historical precedent for future climates that may be characterized by low or zero carbon production. The climate of the LIA has been reconstructed from various proxy records, including tree rings, ice cores, deep ocean and lake sediments, historical accounts, and archaeological data. A summary of these sources relative to the cooling event is presented by [1]. During the period from 1530 to 1850, temperatures decreased by approximately -0.6°C to -1°C. The LIA assumed global dimensions [2]. The cooling was nearly as significant as the current warming trend, but unlike today's warming, the reduction in atmospheric carbon dioxide during the LIA was only -4.6 parts per million by volume (ppmv) (Fig. 1), a small fraction of the more than 100 ppmv increase observed today. Despite this modest decrease, advancing glaciers destroyed communities, devastated crops, and submerged cities under snow and ice. Rivers that are now free-flowing year-round were covered by thick ice in winter. Famine, disease, and social unrest during this time are often attributed to this cooling period. The decade 1691–1700 was one of the coldest in Switzerland over the past five centuries.

The causes of the LIA remain unclear and have been the subject of ongoing research. Proposed causes include volcanic activity and aerosol emissions, changes in solar output and sunspot activity, and changes in ocean currents, such as the North Atlantic Oscillation [3]. Another publication [4] presented an intriguing and relevant explanation, suggesting that the drivers of the LIA were similar to those of past glaciations—specifically, the exchange of cold deep-ocean water with surface waters. Koch et al. [5] concluded that the LIA was primarily the result of an increase in plant and vegetation growth following a population reduction and changes in land use. The cooling period coincided with the discovery of the Americas, which sparked trade between the Old and New Worlds. This exchange included not only goods and livestock but also pathogens and diseases, which decimated nearly 54.5 million people in the Americas alone. As a result, cultivated fields and plantations were abandoned, and vegetation naturally reclaimed the land. Additional ecological shift during LIA is discussed by [6], noting the introduction of horses to the New World and the impact on Native American societies. Natives learned horse breeding, cavalry skills, and used horses to reach distant hunting grounds, leading to a shift from settled agricultural communities to more nomadic lifestyles. This may have contributed to the abandonment of settlements and farmlands, allowing nature to reclaim the land.

The published paper [5] investigated historical, archaeological, population statistics, and field data from the Americas during the LIA and concluded that factors like volcanic aerosols, solar output, or ocean currents were not significant contributors. Instead, they found that the depopulation of the Americas and the subsequent re-growth of plants and vegetation led to a decrease in atmospheric carbon dioxide, which is reflected in the geological record of the LIA (Fig. 1). The authors estimated a reduction of 7-10 ppmv in atmospheric carbon dioxide, which, according to their climate models, contributed to a decrease in surface temperature by approximately -0.15°C. This calculated temperature reduction seems small in comparison to the severity of the event.

This study suggests that even small increases in plant and vegetation inventory, sufficient to reduce carbon dioxide by -4.6 ppmv, can lead to cooling events like the LIA. This occurs because photosynthesis, as a living thermodynamic cycle, inherently drives the growth of plants

when conditions are favorable and no obstacles are present [7]. Depopulation removed human obstacles to plant growth, allowing vegetation to expand and cover abandoned farmlands in the Americas. Vegetation growth is a thermodynamic process that interacts with Earth's global ecology. Photosynthesis, like other thermodynamic processes, requires a medium for heat transfer. For aquatic photosynthesis, this medium is seawater. As vegetation grew, seawater was drawn down from the surface, where photosynthesis occurs, and deep-ocean cold water was brought to the surface, cooling the surface temperature—a process first proposed by [4].

This work demonstrates that the exchange of cold deep-ocean water with surface waters can explain the LIA and past shifts in climate. Such exchanges could potentially occur in both current and future climates. This study is part of a broader research effort to define the thermodynamic interactions between living matter and global ecology. Several related papers have been published and are briefly summarized in this manuscript, which includes theory, data, sample calculations, error analysis, and discussions of the findings. Due to the interdisciplinary nature of the subject, a section titled "Symbols and Abbreviations" has been provided to explain the meaning of the symbols used throughout the work.

2. Background information

Plants and vegetation multiply through photosynthesis, a chemical process limited by the scarcest available resource, as described by Liebig's Law (the Law of the Minimum). The resources include, but are not limited to, sunlight, water, carbon dioxide, nutrients, weeds, pests, and human care. Recently, an additional climatic limiting factor for photosynthesis has been identified by [8]: the difference between the air dry bulb temperature (T_{db}) and the air wet bulb temperature (T_{wb}), which arises from thermodynamic analysis of photosynthesis as a Carnot thermodynamic cycle. If $T_{db}=T_{wb}$, plants cannot grow, regardless of the abundance of other resources.

A basic explanation for this is that, like other processes, photosynthesis requires the rejection of excess heat, typically through plant transpiration. If this heat rejection is blocked, photosynthesis will not occur. When $T_{db}=T_{wb}$, air relative humidity reaches saturation (100%), and plant transpiration is inhibited, preventing photosynthesis from proceeding. Therefore, the interaction between vegetation, climate, and Earth's ecology can be determined with reasonable accuracy: Climate, in this context, involves air dry bulb temperature, air wet bulb temperature, air humidity, surface water evaporation, and heat exchange. The physics that unifies these processes—air psychrometry—is an established field of knowledge. Additionally, the growth and decay of plants and vegetation can be monitored by measuring the variation in atmospheric carbon dioxide concentrations, which can be done with great accuracy [9].

Therefore, plants and vegetation require a heat reservoir, a cold reservoir, and a medium for heat transfer, typical for thermodynamic processes. Air serves as the medium of heat transfer for terrestrial photosynthesis, while seawater serves as the medium for aquatic photosynthesis. Areas covered by trees and vegetation experience slow, dense, and cool air produced by terrestrial photosynthesis. For dense forests, such as rainforests, the flow of air may be large enough to create a local climate [10]. Likewise, aquatic photosynthesis relies on seawater as the medium for heat transfer. During vegetation growth, seawater flows downward from the warm surface, where green matter and sunlight coexist, to the deep ocean. The displaced cold deep-ocean water reaches sea surface, causing a decrease in surface temperature. In contrast, deforestation and decay of plants and vegetation prevent deep-ocean water from reaching the

surface. This process potentially explains how deep-ocean water and surface water may have been exchanged, which is a proposed prerequisite for past climate variations, as discussed in the introduction section.

The thermohaline circulation connects the deep ocean with surface water. Cold water from the deep southern oceans can transit the entire ocean mixed layer in about 25 years [11], which is a relatively short period compared with the duration of the LIA or past glaciations. Therefore, the proposed process of deep-ocean water exchange with the surface during the LIA and past glaciations appears to be a sensible and realistic hypothesis. This work demonstrates that plants and vegetation may have been the agents facilitating the heat exchange between the deep ocean and the surface.

Furthermore, photosynthesis as a thermodynamic cycle complies with the laws of thermodynamics, specifically the conservation of energy. The proposal of heat exchange between the deep ocean and the surface is in compliance with these laws, as heat is exchanged within the earth. Accordingly, the interactions between plants and vegetation and ocean currents are parameterized in this work. A theoretical analysis of these interactions is conducted, and the final governing equations are derived. These equations are then tested for agreement with available data and observations, and they appear to pass this test. It is therefore concluded that the growth of plants and vegetation may have facilitated the transfer of cold deep-ocean water to the surface, thus contributing to the Little Ice Age.

3. Theory and analysis

3.1 Photosynthesis as a thermodynamic cycle

Figure 2 illustrates terrestrial photosynthesis as a Carnot thermodynamic cycle, based on [8]. The surrounding warm air of plants and vegetation, at the air dry bulb temperature T_{db}, serves as the heat reservoir, while the air space enclosed by plants and vegetation, at the air wet bulb temperature T_{wb}**,** serves as the cold reservoir. The thermal efficiency of photosynthesis is: $\eta=1-(T_{wb}/T_{db})^{0.5}$, where T_{db} and T_{wb} are measured in degrees Kelvin. Global terrestrial photosynthesis, on the other hand, has surface water as the heat reservoir and the atmosphere as the cold reservoir. Air is the medium of heat transfer, and the excess heat from photosynthesis is rejected to the atmosphere through plant transpiration.

Aquatic photosynthesis also operates as a thermodynamic cycle (Fig. 3), similar to terrestrial photosynthesis, but with water as the medium of heat transfer. Surface water serves as the heat reservoir. Unlike terrestrial photosynthesis, aquatic photosynthesis does not transpire and therefore has no access to the cold reservoir, which is the atmosphere. However, it is coupled with terrestrial photosynthesis, and the excess heat from aquatic photosynthesis is channeled to the atmosphere through the air medium of heat transfer of terrestrial photosynthesis.

Aquatic and terrestrial photosynthesis share the same heat and cold reservoirs—surface water and atmosphere, respectively. As a result, they have an equal inventory of green matter, seasonal efficiency of photosynthesis, and thermodynamic driving force [12]. This driving force is the difference between the air dry bulb and wet bulb temperatures, T_{db}-T_{wb}. During the day, solar heat absorbed by the land intensifies, and a temperature difference, T_{db}-T_{wb}, materializes. At the same time, the solar energy absorbed by seawater decreases exponentially with depth,

creating a temperature difference, equivalent to T_{db}-T_{wb}, at the sea surface, which becomes available for aquatic photosynthesis. Between points 1 and 2, an amount of solar heat equal to dQ_{HA} is gained isothermally at T_{db} by the seawater medium of heat transfer. The medium then cools isentropically (2-3) to T_{wb}, and the chemical energy of aquatic green matter, $dQ_G/2$, is produced—equal to half of the global biomass produced, dQ_G. Between points 3 and 4, the medium undergoes isothermal compression, and the heat dQ_{CA} is rejected to the cooler seawater below the surface by the mass flow of the heat transfer medium, $M_{PH}(t)$, as shown in Fig. 4. The mass flow is replaced by an equal volume of warm seawater at the surface, and the thermodynamic cycle repeats. A net flow $M_{PH}(t)$ is thus established as long as aquatic photosynthesis continues to grow.

3.2 Photosynthesis-thermohaline circulation interaction

Referring to Fig. 4, which shows the co-existence of photosynthesis and thermohaline circulation [13, 14]: photosynthesis occupies the ocean mixed layer, where solar radiation and chlorophyll coexist. Without aquatic photosynthesis, the flow of the seawater heat transfer medium, $M_{PH}(t)$, is absent. The solar heat to the sea surface and the Earth's internal heat to the ocean floor are balanced by sea surface evaporation. These energy streams are shown as dashed lines because they cancel each other out and do not alter the heat and mass balance of the ocean mixed layer. When $M_{PH}(t) = 0$, the thermohaline circulation would have a steady and constant flow, M, below the surface. At the sea surface (or ocean mixed layer), the temperature of the thermohaline brine decreases from south to north due to surface evaporation. When the surface brine temperature, T_N, of the northern oceans is equal to or slightly less than the temperature of the deep ocean, T_O, the surface brine sinks by gravity onto the ocean floor. Nearly seventy percent of the Earth's internal heat to ocean, 0.70 Q_{IN}, is absorbed by the thermohaline brine as it adheres to the ocean floor. The rising, slightly warmer brine from the southern oceans at temperature T is brought to the surface, and most of the Earth's internal heat gained by the thermohaline circulation is removed by surface evaporation. The brine temperature decreases from T to T_N, and the thermohaline brine cycle repeats.

When aquatic photosynthesis grows, the medium of heat transfer, $M_{PH}(t)$, is established (Fig. 4). It removes a volume of warm water at surface temperature T_S from the thermohaline circulation. Simultaneously, an equal volume of cold deep-ocean water at temperature T_O is admitted into the mass of the circulated brine. If this process continues for an extended period, intensive sea surface cooling and glaciation may occur. The longer the duration of green matter growth, the colder the surface temperature.

3.3 Parameterization of glaciation temperature

When plants and vegetation grow, the global increase in the inventory of plants and vegetation, dQ_G, can be estimated by conducting a heat and mass balance of carbon dioxide in the atmosphere. All that is required is the decrease in the atmospheric carbon dioxide content:

$$dQ_G = -7.07 \times 10^{19} \times d(ppmv) \quad (1)$$

Where

dQ_G=Annual increase in the chemical energy of global photosynthesis, J yr^{-1}.

d(ppmv)=Annual decrease in the concentration of carbon dioxide in the atmosphere in parts per million by volume.

The above relationship is obtained from equation 5 of [12]. Basic Carnot thermodynamic relationships relative to Figures 2 and 3 can be found in typical textbooks on thermodynamics, such as [15]. Therefore

$$dQ_{HT} = dQ_{HA} = [(dQ_G/2)/\eta] \quad (2)$$

$$M_{PH} = dQ_{HA}/[C_{PW} \times (T_{db} - T_{Wb})] \quad (3)$$

$$\eta = 1 - (T_{wb}/T_{db})^{0.5} \quad (4)$$

Where

dQ_{HT}=Heat supply by the heat reservoir, surface water, of terrestrial photosynthesis, J yr^{-1}.

dQ_{HA}=Heat supply by the heat reservoir, surface water, of aquatic photosynthesis, J yr^{-1}.

$dQ_G/2$=Chemical energy produced by aquatic photosynthesis, half of the total dQ_G, J yr^{-1}.

η=Seasonal efficiency of terrestrial photosynthesis thermodynamic cycle, dimensionless.

M_{PH}=Mass flow of aquatic photosynthesis medium of heat transfer, seawater, kg yr^{-1}.

C_{PW}=Specific heat of seawater, J $kg^{-1}°C^{-1}$.

T_{db}=Average land surface air dry bulb temperature, °K.

T_{Wb}=Average land surface air wet bulb temperature, °K.

Referring to Fig. 4, aquatic photosynthesis occupies the ocean mixed layer, where solar radiation and chlorophyll coexist. If photosynthesis is absent, the flow of the heat transfer medium, $M_{PH}(t)=0$. The mass flow rate of the thermohaline circulation, M, would be constant, and the ocean mixed layer would be around equilibrium, represented by:

$$d[M_S(t)\, C_{PW}\, T_S(t)]/dt = 0 \quad (5)$$

Where $M_S(t)$ and $T_S(t)$ are the mass and average temperature of the ocean mixed layer (in kg and °C, respectively).

When plants and vegetation grow, the flow of the heat transfer medium $M_{PH}(t)$ materializes. An amount of heat (enthalpy) equivalent to $M_{PH}(t)\, C_{PW}\, [T_S(t) - T_{S*}]$ exits the ocean mixed layer, and an amount of heat (enthalpy) equivalent to $M_{PH}(t)\, C_{PW}\, [T_O - T_{S*}]$ enters the ocean mixed layer. Where T_O is the temperature of the deep ocean water, °C, and T_{S*} is a reference sea temperature, °C. The heat balance of the ocean mixed layer follows:

$$d[M_S(t)\, C_{PW}\, T_S(t)]/dt = M_{PH}(t)\, C_{PW}\, T_O - M_{PH}(t)\, C_{PW}\, T_S(t) \quad (6)$$

$$d[M_S(t)\, T_S(t)]/dt + M_{PH}(t) T_S(t) = M_{PH}(t)\, T_O \quad (7)$$

Equation (7) is a first-order differential equation in terms of surface temperature $T_S(t)$. It can be solved provided that the functions $M_{PH}(t)$ and $M_S(t)$ are known. The mass flow of the heat transfer medium, $M_{PH}(t)$, is variable depending on the nature of living green matter. Additionally, $M_S(t)$ varies with the depth of the ocean mixed layer, which increases over time.

As surface temperature decreases, air circulation intensifies to remove surface water evaporation at lower water vapor pressure, resulting in more surface water mixing. For simplicity, their average values, M_{PH} and M_S, for the entire glacial period may be used

$$dT_S(t)/dt+[M_{PH}/M_S]\ T_S(t)=[M_{PH}/M_S]\ T_O \quad (8)$$

Solution of Eq. (8) gives

$$T_S\,(n)=(T_{S0}-T_O)\ Exp[-(M_{PH}/M_S)\ x\ n)]+T_O \quad (9)$$

$$\Delta T_S=T_S(n)-T_{S0} \quad (10)$$

Where

T_S (n)=Sea surface temperature after n years, °C

T_{S0}=Initial sea surface temperature, °C.

n=Duration of the glacial or cooling period, years.

ΔT_S=Total decrease in surface temperature in n years, °C.

As discussed in the background section, the residence time of the thermohaline circulation in the ocean mixed layer is 25 years. Therefore, the actual cooling of the surface lags the decrease in the concentration of carbon dioxide by nearly 25 years. This is a small period compared with the duration of the LIA event that continued for over 200 years (Fig. 1), or ice ages that lasted millennia.

4. Data analysis and method

To calculate the flow rate of the aquatic photosynthesis medium of heat transfer (M_{PH}), the required parameters are air dry temperature, air wet bulb temperature, and the seasonal efficiency of photosynthesis. According to the technical summary of the Intergovernmental Panel on Climate Change [16], the observed total increase in global surface temperature through 2020 was 1.09°C (with a range of 0.95 to 1.2°C). The preindustrial temperature is assumed to have been approximately 13.7°C. Using the psychrometric chart [17] and the current global average air relative humidity of 60%, the preindustrial air relative humidity was between 65% and 69%. With an average of 67% and an air dry bulb temperature of 13.7°C, the air wet bulb temperature (T_{wb}) during the Little Ice Age (LIA) was approximately 10.44°C. The thermal efficiency of photosynthesis is given by eq. (4):

$$\eta=1-[(10.44+273.15)/(13.7+273.16)]^{0.5}= 0.0057$$

According to the source data in Fig. 1 [18], the concentration of carbon dioxide in the atmosphere in the year 1538 was approximately 281.36 ppmv. By 1628, this concentration had decreased to 276.76 ppmv. Proxy data analysis indicates that the observed decrease in surface temperature during the LIA was between -0.6°C and -1°C [1, 2, 3, 19].

The physical and geometrical parameters of Earth's surface and ocean can be obtained from [20]. The surface area of Earth (A_S) is 5.10×10^{14} m², with the ocean covering nearly 70% of this area. Psychrometric relationships of air-water mixtures are available from [17]. The physical properties of brine, such as density (δ) and specific heat (C_{PW}), are provided by [21].

The density of seawater is 1 048 kg/m³, and its specific heat is 3 980 J/(kg·°C). The average depth of the ocean mixed layer (h) is approximately 95 m [22].

The ideal solution methodology is to conduct the calculations on an annual basis. By knowing the annual decrease in the concentration of carbon dioxide in the atmosphere, the annual production of green matter (dQ_G) can be determined. The seasonal efficiency of photosynthesis and the difference between air dry and wet bulb temperatures allow for the determination of the annual flow rate of the heat transfer medium (M_{PH}) using Eqs. (1) through (4). In the following year, the annual decrease in surface temperature is calculated using Eqs. (9) and (10). The seasonal efficiency of photosynthesis and the difference between air dry and wet bulb temperatures are then recalculated using air-water psychrometric relationships or psychrometric charts, and the calculations are repeated through the final year of the glacial period. For simplicity, average values of the seasonal efficiency of photosynthesis and the temperature difference between air dry and wet bulb temperatures may be used for the entire glacial period.

Finally Large Language Models (LLMs) have been occasionally consulted for concepts' originality and merit, as well as AI assisted copy editing for text grammar, readability, and flow. These models include Ask Ai and ChatGPT. The author generated all original texts, and the final edited texts reflect the original work.

5. Sample calculations and error analysis

Given the LIA initial conditions: year 1538. From the data section, the initial surface temperature T_{S0}=13.7 °C; T_{db}-T_{Wb}=13.7-10.44=3.26 °C; the seasonal efficiency of photosynthesizes η=0.0057; the concentration of carbon dioxide in the atmosphere=281.36 ppmv; the depth of the ocean mixed layer h= 95 m; the specific heat of sea water C_{PW}=3 980 J kg^{-1} $°C^{-1}$; the temperature of the deep ocean water, T_O≈3.5 °C.

Given the LIA final conditions: year 1628. The concentration of carbon dioxide in the atmosphere=276.76 ppmv.

The decrease in the content of carbon dioxide in the atmosphere is equal to 276.76-281.36=-4.60 ppmv. The number of years n=1628-1538=90.

The total chemical energy of vegetation growth ΔQ_G=-7.07 x 10^{19} (-4.6)=3.25 x 10^{20} J, Eq. (1).

The average annual chemical energy of vegetation growth dQ_G=ΔQ_G/n=3.25 x 10^{20}/90=3.61 x 10^{18} J yr^{-1}. Aquatic photosynthesis produced half of this energy, dQ_G/2= 1.81 x 10^{18} J yr^{-1}.

dQ_{HA}=(dQ_G/2)/η=1.81 x 10^{18}/0.0057=3.17 x 10^{20} J yr^{-1}, Eq. (2).

M_{PH}=[(dQ_{HA}]/[C_{PW} x (T_{db}-T_{Wb})]= 3.17 x 10^{20}/(3 980 x 3.26)=2.44 x 10^{16} kg yr^{-1}, Eq. (3).

M_S=0.7A_S x h x δ=0.7 x 5.10 x 10^{14} x 95 x 1 048=3.55 x 10^{19} kg.

$T_S(n)$=(T_{S0}-T_O) Exp[-(M_{PH}/M_S) x n]+T_O=(13.7-3.5) Exp [-2.44 x 10^{16}/(3.55 x 10^{19}) x 90]+3.5=13.09, Eq. (9).

ΔT_S=$T_S(n)$-T_{S0} =13.09-13.7=-0.61 °C, Eq. (10).

For the last glacial period, the same calculations may be repeated. Based on [23, Fig. 3], the beginning climatic conditions of the last glacial period may be assumed to be comparable to those of preindustrial era. The final conditions are extremely cold climates, similar to those of the Last Glacial Maximum. The air relative humidity approaches saturation, and T_{db}≈T_{Wb}. The seasonal efficiency of photosynthesis thus assumed negligible values.

Given initial conditions: year -120 000 Before Present. The initial surface temperature T_{S0}=13.7 °C; T_{db}-T_{Wb}=3.26 °C; the seasonal efficiency of photosynthesizes η=0.0057; the

concentration of carbon dioxide in the atmosphere=281.36 ppmv; the depth of the ocean mixed layer h= 95 m; the specific heat of sea water C_{PW}=3 980 J kg^{-1} $°C^{-1}$; the temperature of the deep ocean water, T_O≈3.5 °C.

Given final conditions: year -20 000 Before Present; T_{db}-T_{Wb}≈0; the seasonal efficiency of photosynthesizes η≈0; the concentration of carbon dioxide in the atmosphere=180 ppmv.

Glaciation average conditions: T_{db}-T_{Wb}=(3.26+0)/2=1.63; Number of years n=100 000; the average efficiency of photosynthesis (0.0057+0)/2=0.00285.

The above calculations for LIA may be repeated:

The total chemical energy sequestered by green matter ΔQ_G=-7.07 x 10^{19} (180-281.36)= 7.17 x 10^{21} J, Eq. (1).

The annual chemical energy of vegetation growth dQ_G=ΔQ_G/n=7.17 x 10^{21}/100 000= 7.17 x 10^{16} J yr^{-1}. Aquatic photosynthesis produced half of this energy, dQ_G/2= 3.58 x 10^{16} J yr^{-1}.

dQ_{HA}=(dQ_G/2)/η=3.58 x 10^{16}/0.00285=1.26 x 10^{19} J yr^{-1}, Eq. (2).

M_{PH}=[(dQ_{HA}]/[C_{PW} x (T_{db}-T_{Wb})]= 1.26 x 10^{19}/(3 980 x 1.63)=1.94 x 10^{15} kg yr^{-1}, Eq. (3).

M_S=0.7A_S x h x δ=0.7 x 5.10 x 10^{14} x 95 x 1 048=3.55 x 10^{19} kg.

T_S (n)=(T_{S0}-T_O) Exp[-(M_{PH}/M_S) x n]+T_O=(13.7-3.5) Exp [-1.94 x 10^{15}/(3.55 x 10^{19}) x 100 000]+3.5=3.54, Eq. (9).

ΔT_S=T_S(n)-T_{S0}=3.54-13.7=-10.16 °C, Eq. (10).

For LIA error analysis calculation, the absolute value of the error of a variable x is indicated by Δx. The relative error, Δx/x, is denoted by εx. The maximum value of the error is indicated by Max ε. The absolute value of the error in the calculated surface temperature variation, ΔT_S, depends on the accuracy of the physical parameters of Eq. (9) as well as the number of years in consideration n. The absolute value of the error in the chemical analysis of carbon dioxide is less than 0.01 ppmv [9]. Therefore, the errors in the calculated chemical energy of photosynthesis, dQ_G, seasonal efficiency of photosynthesis, η, and dQ_{HA} may be neglected. The estimated absolute value of the error in global temperature measurement could be nearly equal to 0.048°C [24]. Referring to Eq. (3), the following may apply:

ΔM_{PH}=[{C_{PW} x (T_{db}-T_{Wb})} Δ(dQ_{HA})- (dQ_{HA}) C_{PW} x (ΔT_{db}-ΔT_{Wb})]/[C_{PW} x (T_{db}-T_{Wb})]^2

The value of Δ(dQ_{HA}) is negligible as discussed earlier. Therefore

Max $\Delta M_{PH}/M_{PH}$=[0-(dQ_{HA})/M_{PH} x C_{PW} x ($\Delta T_{db+}\Delta T_{Wb}$)]/[$C_{PW}$ x (T_{db}-T_{Wb})]^2

Max εM_{PH}=(dQ_{HA})/M_{PH} x ($\Delta T_{db+}\Delta T_{Wb}$]/[$C_{PW}$ x (T_{db}-T_{Wb})^2]

Max εM_{PH} =±(3.17 x 10^{20})/2.44 x 10^{16} x (0.048+0.048)]/[3 980 x 3.26^2]

Max εM_{PH}=±0.03, or ±3.0%.

Equation (9) gives

ΔT_S=(T_{S0}-T_O)Exp[-M_{PH}/M_S x n] x Δ(-M_{PH}/M_S)(n)+Exp[-M_{PH}/M_S x n][ΔT_{S0}-ΔT_O]+ΔT_O

M_S/M_{PH}=3.55 x 10^{19}/2.44 x 10^{16}=1 454.92; M_{PH}/M_S =6.87 x 10^{-4}.

Δ(M_{PH}/M_S)=(M_S ΔM_{PH} - M_{PH} ΔM_S)/M_S^2=(ΔM_{PH}/M_{PH}- ΔM_S/M_S)/(M_S/M_{PH})=(εM_{PH} +εM_S)/1 454.92=(0.03+0.2)/(1 454.92)=1.58 x 10^{-4}

Max ΔT_S=±(13.7-3.5) Exp [-6.87 x 10^{-4} x 90] x 6.87 x 10^{-4} x 90+Exp[-6.87 x 10^{-4} x 90] x (0.048+0.048) +0.048=±0.20 °C.

Max ε ΔT_S= ΔT_S/T_S=±0.20/[(3.5)]=±0.056; The maximum relative error in the calculated temperature decrease is nearly±5.6%.

6. Discussion and conclusions

The Food and Agriculture Organization of the United Nations [25] reports that deforestation since early human history has reached nearly 50%. “There has been a relationship between population growth, increased demand for agricultural land, and forest loss dates back thousands of years. Forests have sometimes re-established naturally as deforestation pressures have eased. Archeological and historical records reveal that the decrease in forest size is associated with population growth and demand for crops and grazing land. In locations of the world that had experienced severe disease and population decline, forests re-grew again.”

About 5 000 years ago, the world population was nearly five million [26]. When farming was invented approximately 8 000 years ago, the human population was likely around five million or less. This small society of humans appears to have mitigated a cooling cycle, resulting in the longest interglacial period in the last 400 000 years [23]. By 1500 AD, the world population had grown to about 500 million, of which 54.5 million were decimated by diseases, as discussed in the Introduction. This loss of population was significant, particularly compared to human societies similar to those that existed 8 000 years ago. Land reforestation during the Little Ice Age (LIA) occurred relatively quickly, with vegetation growth at a rate of -0.03 ppmv of carbon dioxide annually—four to five times greater than observed during the last four glacial periods. Conditions conducive to a glaciation during the LIA may potentially have existed. The growth of plants and vegetation following the depopulation of the Americas appears to be a plausible cause of the Little Ice Age, based on this historical narrative.

The sample calculations support this historical narrative. The calculated decrease in surface temperature is -0.61±0.03°C for a reduction in the concentration of carbon dioxide by -4.6 ppmv. A decrease of -7 to -10 ppmv would result in a depression in surface temperature between -0.92±0.05°C and -1.29±0.07°C, respectively, which aligns with the estimated -0.6°C to -1°C. Similarly, for the last glaciation period, the calculated decrease in surface temperature of -10.16±0.57°C compares well with the observed average decrease of -10.56°C during the last four glacial cycles [23]. The calculation error is less than 5.6%. This method is reasonably accurate, as anticipated earlier in the background section. Therefore, the natural reforestation of abandoned lands following the depopulation of the Americas likely contributed to the Little Ice Age. The hypothesis that deep ocean water exchange with sea surface could have influenced past climatic changes is further supported by both theory and observations.

These conclusions offer valuable insights for the present and future of Earth's ecology. The Industrial Revolution, which began around 1750 AD, marked the end of the Little Ice Age (Fig. 1). Since then, the world population has increased rapidly, driven by large-scale mechanized deforestation and farming of cleared land. Deforestation, in contrast to photosynthetic growth and surface greening, contributes to surface warming. Currently, deforestation and surface greening have contributed 22.85% and -12.84%, respectively, to the total heat added to Earth's surface [12]. As of now, deforestation has outpaced surface greening, and it is likely that deep ocean cold water is not transferring to the surface. However, this could change as deforestation approaches its maximum value. At this point, when the world population nears Earth's maximum carrying capacity, cold climates similar to the LIA—or even colder—could potentially emerge.

The influence of plants and vegetation on ice ages is complex, as shifts in vegetation patterns and dynamics can affect the Earth’s climate system. These changes can lead to severe climates, which may have devastating effects on agriculture and ecosystems that rely on stable

environmental conditions. As such, managing future climate conditions will be crucial for preserving both food production and global ecological health.

7. References

1. Fagan, B. *The Little Ice Age*, *How Climate Made History 1300-1850* (Basic Books, New York, NY, USA, 2002) 272 p.

2. Grove, J. M. *Little Ice Ages, Ancient and Modern*, Second Edition, (Rutledge, New York, NY, USA, 2004) 718p.

3. Mann, M. E. Little Ice Age in *Encyclopedia of Global Environmental Change* (eds. MacCracken, M. C. & Perry, J. S.) (John Wiley & Sons, Ltd., Manchester, UK, 2002).

4. Broecker, W. S. Was a change in thermohaline circulation responsible for the Little Ice Age. *PNAS* **97** (4), 1339-1342 (2000). https://doi.org/10.1073/pnas.97.4.1339

5. Koch, A., Brierley, C., Maslin, M. M. & Lewis, S. L. Earth System Impacts of the European arrival and Great Dying in the Americas after 1492. *Quaternary Science Review* **207**, 13-36 (2019). https://doi.org/10.1016/j.quascirev.2018.12.004

6. Duval, K. *Native Nations* (Random House, Penguin Random House LLC, New York, NY, USA, 2024) 718 p.

7. Vernadsky, V. I. The Biosphere (Springer-Verlag, New York, NY, USA, 1998) 192 p.

8. Swedan, N. Photosynthesis as a thermodynamic cycle. *Heat and mass transfer* **56**, 1649-1658 (2020). doi.org/10.1007/s00231-019-02768-x

9. Keeling, C. D. et al. Atmospheric carbon dioxide variations at Mauna Loa Observatory, Hawaii. *Tellus* **6**, 538-551 (1976). https://doi.org/10.1111/j.2153-3490.1976.tb00701.x

10. Wright, J. S., Fu, R., Worden, J. R. & Lei Y. Rainforest-initiated wet season onset over the Southern Amazon. *PNAS* **114**, (32), 8481-8486 (2017). https://doi.org/10.1073/pnas.1621516

11. Becker, P. & Björk, G. Residence times in the upper Arctic Ocean. *Journal of Physical Research: Oceans* **101** (12), 28377-28396 (1996). Https://doi.org/10.1029/96JC02641

12. Swedan, N. H. Thermodynamic Analysis of Climate Change. *Entropy* **25**, 72 (2023). https://doi.org/10.3390/e25010072

13. Toggweiler, J. R. & Key, R. M. Thermohaline Circulation in *Encyclopedia of Ocean Sciences* (eds. Thrope, S. A. & Turekian, K. K.) 2941-2947 (Academic Press, Cambridge, MA, USA, 2001). https://doi.org/10.1006/rwos.2001.0111

14. Kurtz , B. E. An Electrical Analogy Relating the Atlantic Multidecadal Oscillation to the Atlantic Meridional Overturning Circulation. *PLoS ONE* **9**(6) (2014). http://dx.doi.org/10.1371/journal.pone.0100306

15. Liley, P. E. Thermodynamics in *Mark's Standard Handbook for Mechanical Engineers*, Tenth Edition (eds. Avallone, E. A. & Baumeister, T. III) 4-2 to 4-12 (McGraw-Hill, New York, USA, 1996).

16. Arias, P.A. et al. Technical Summary in *Climate Change 2021, The Physical Science Basis*, *Contribution of Working Group I to the Sixth Assessment Report of the Intergovernmental Panel on Climate Change* (eds. Masson-Delmotte, V. P. et al.) 33-144 (Cambridge University Press Cambridge, UK, and New York, NY, USA, 2021). https:/doi,org/10.1017/9781009157896.002.

17. Bognoli, E., Norris, R. W., Flynn, T. M. & Timmerhaus, K. D. Psychrometry in *Perry's Chemical Engineers Handbook*, Sixth Edition (eds. Crawford, H. B. & Eckes, B. E.) 12-3, 12-13 (Mc Graw-Hill, New York, NY, USA, 1984).

18. NOAA. Paleoclimates, ice core data, carbon dioxide (National Oceanic and Atmospheric Administration, Manchester MA, USA, website accessed on January 15, 2025). https://www.ncei.noaa.gov/access/paleo-search/

19. Jackson, S. T. & Rafferty, J. P. *Littl Ice Age* (Encyclopedia Britannica, Chicago, IL, USA, website accessed January 10, 2024). https://www.britannica.com/science/Little-Ice-Age

20. Fleagle, R. G. & Businger, J. A. *An Introduction to Atmospheric Physics*, Second Edition (Academic Press, New York, NY, USA, 1980) 432 p.

21. Liley, P. E., Reid, R. C. & Buck, E. Physical and Chemical Data in *Perry's Chemical Engineers Handbook*, Sixth Edition (eds. Crawford, H. B. & Eckes, B. E.) 3-148 (Mc Graw-Hill, New York, NY, USA, 1984).

22. de Boyer Montégut, C., Madec, G., Fischer, S. A., Lazar, A. & Iudicone, D. Mixed layer depth over the global ocean: An examination of profile data and profile-base climatology. *J Geophys. Res.* **109**: C12003 (2004). doi: 10.1029/2004JC002378

23. Petit, J. R. et al. Climate and atmospheric history of the past 420,000 years from the Vostok ice core, Antarctica. *Nature* **399**, 429–436 (1999). doi:10.1038/20859

24. Jones, P. D., New, N., Parker, D. E., Martin, S. & Rigor, I. G. Surface air temperature and its changes over the last 150 years. *Review of Geophysics* **37** (2), 173-199 (1999). doi: 10.1029/1999RG900002

25. FAO. *State of the World's Forests. Forests and Agriculture: Land-use challenges and opportunities* (Food and Agriculture Organization of the United Nations, Rome, Italy, 2016). http://www.fao.org/3/a-i5588e.pdf

26. Cain, M. L., Bowman, W. D. & Hacker, S. D. Ecology, Third Edition (Sinauer Associates, Inc., Sunderland MA, USA, 2014), 596 p.

8. Acknowledgements: The Author acknowledges that this manuscript is entirely authentic and genuine and the entire work has been prepared by the Author. This manuscript is not currently being considered for publication by other journals. No data has been fabricated or manipulated. All data are accessible online using the links provided in the references section. Furthermore, the Author has no conflict of interest as a result of this publication. This publication is funded by the

9. Competing Interest: The author declares no competing interests with respect to the research, authorship, and publication of this manuscript.

10. Author contributions: The author, Nabil Swedan, produced the entire work including original text and figures.

11. Data availability. No new data. The data is readily available online by the links provided under references

12. Figure legends

Fig. 1. Concentration of carbon dioxide in the atmosphere in part per million by volume (ppmv) versus time during the Little Ice Age. Source (NOAA, 2025).

Fig. 2. A schematic representation of the global terrestrial photosynthesis as an ideal Carnot heat engine on the entropy-temperature diagram. dQ_{HT}=heat supply at the temperature of the heat reservoir, surface water, J; dQ_{CT}=heat rejected to the cold reservoir, the atmosphere, J; $dQ_G/2$=chemical energy produced by terrestrial photosynthesis, J; T_{db}=global average air dry bulb temperature, °K; T_{wb}=global average air wet bulb temperature, °K; Thermal efficiency of terrestrial photosynthesis $\eta=1-(T_{wb}/T_{db})^{0.5}$; $dQ_G/2=dQ_{HT}-dQ_{CT}=\eta\, dQ_{HT}$.

Fig. 3. A schematic representation of aquatic photosynthesis as an ideal Carnot heat engine on the entropy-temperature diagram. dQ_{HA}=heat supply at the temperature of the heat reservoir, surface water, J; dQ_{CA}=heat flow to the deeper and cooler sea water, J; $dQ_G/2$=chemical energy produced by aquatic photosynthesis, J; T_{db}=global average air dry bulb temperature, °K; T_{wb}=global average air wet bulb temperature, °K; Thermal efficiency of aquatic photosynthesis $\eta=1-(T_{wb}/T_{db})^{0.5}$; $dQ_G/2=dQ_{HA}-dQ_{CA}=\eta\, dQ_{HA}$.

Fig. 4. A schematic representation of the interaction between aquatic photosynthesis and the ocean's thermohaline circulation. Q_{SL}=annual solar heat exchanged with sea surface water, J yr^{-1}; Q_E=annual latent heat removed by surface evaporation, J yr^{-1}; $M_S(t)$=Mass of the ocean mixed layer, kg; Ts(t)=sea surface temperature, °C; M=mass flow of the thermohaline circulation, kg yr^{-1}; T=temperature of the thermohaline brine of the southern oceans, °C; M_{PH}=mass flow of aquatic photosynthesis seawater medium of heat transfer, kg yr^{-1}; T_N=temperature of the falling thermohaline brine at the surface of the northern oceans, °C;T_O=temperature of the deep ocean water, °C; 0.7 Q_{IN}=Earth's internal heat to the ocean floor, J yr^{-1}.

13. Figures

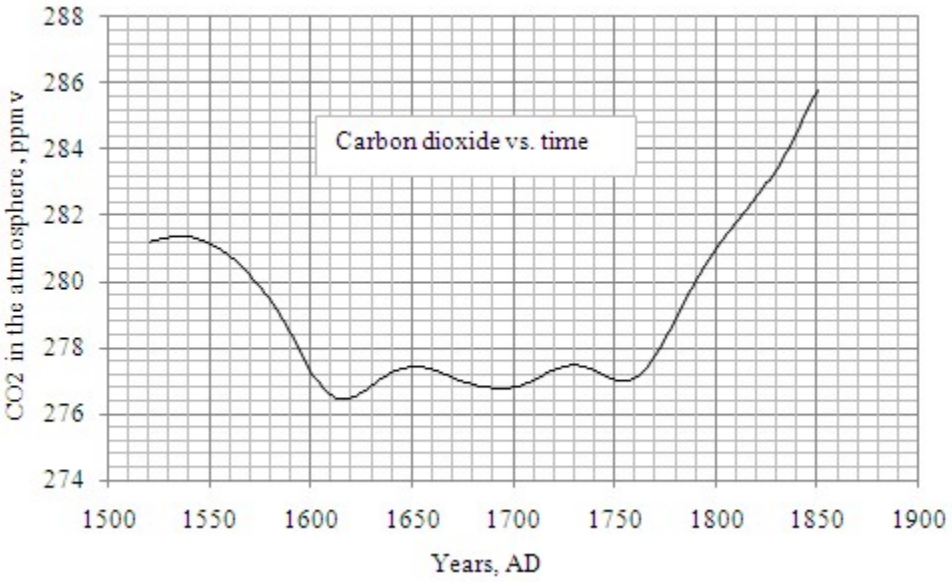

Fig. 1

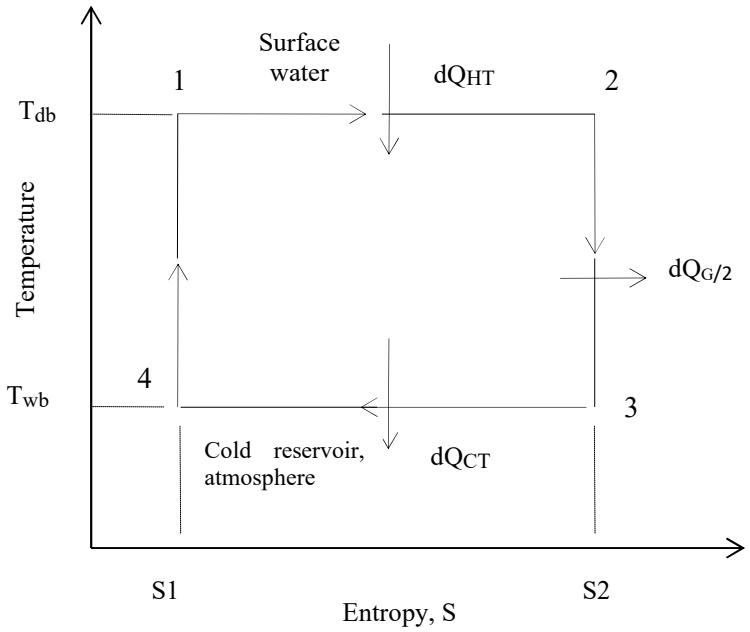

Fig. 2

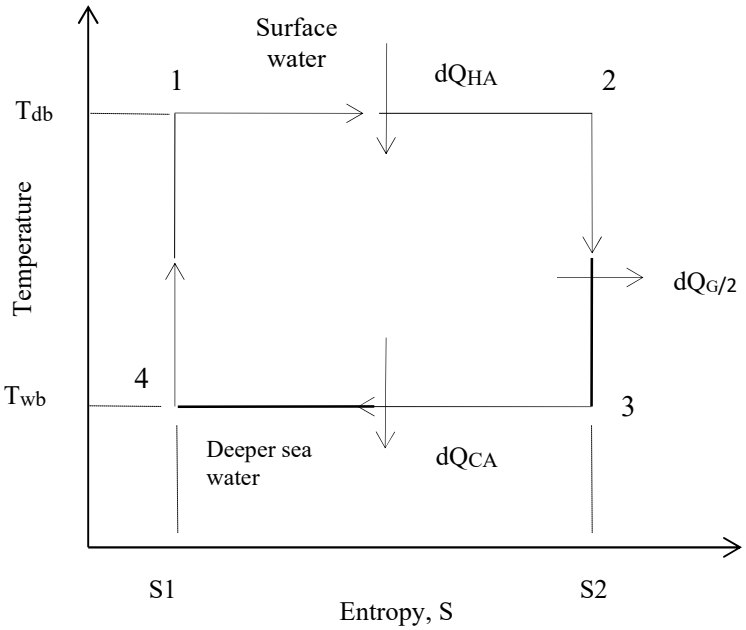

660 Fig. 3

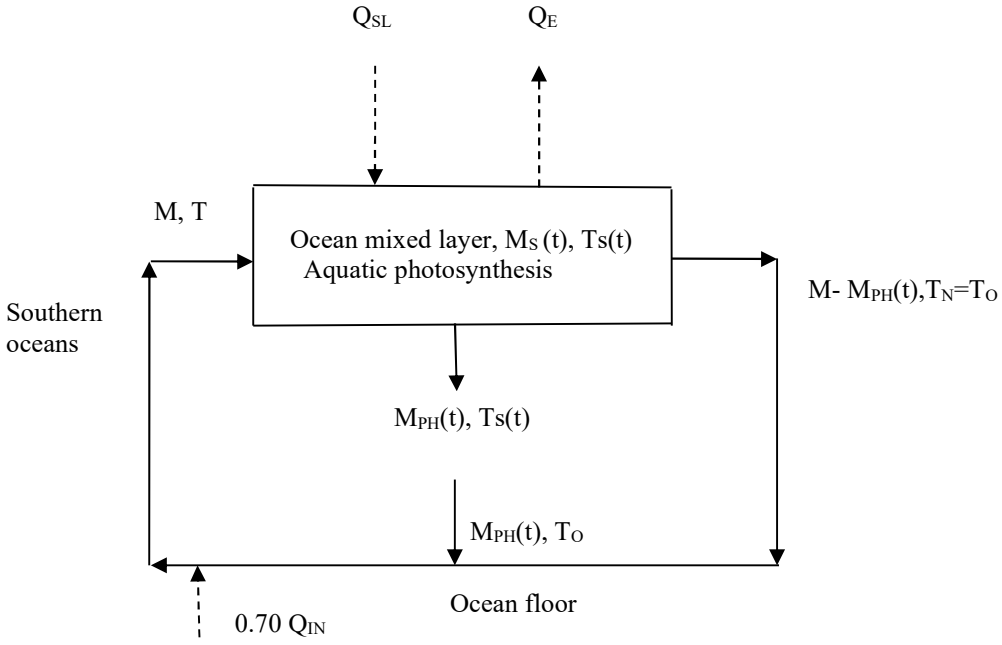

665 Fig. 4

14. Symbols and Abbreviations

A_S	Earth's surface area, m^{-2}
°C	Degrees centigrade
C_{PW}	Specific heat of sea water, J kg^{-1} $°C^{-1}$
d	A symbol denotes infinitesimal variation
Δ	A symbol denotes cum. difference, variation, or absolute value of error
Δx	Absolute value of calculated or measured parameter x
ε	Relative error of a quantity, Δx/x
δ	Density of sea water, kg m^{-3}
dQ_G	Variation in the global chemical energy of photosynthesis, J
ΔQ_G	Total variation in the chemical energy of photosynthesis in n years, J
dQ_H	Heat supply by the heat reservoir, J yr^{-1}
dQ_C	Heat rejected to the cold reservoir, J yr^{-1}
Exp (x)	Exponential function equivalent to e^x
h	Depth of the ocean mixed layer, m
J	Joule
kyr	One thousand years
LIA	Little Ice Age
M	Mass flow rate of the thermohaline circulation, kg yr^{-1}
Ma	Million years
M_S	Mass of the ocean mixed layer at surface, kg
M_{PH}	Mass flow rate of aquatic photosynthesis medium of heat transfer, sea water, kg yr^{-1}
n	Number of years
η	Thermal efficiency of seasonal photosynthesis, dimensionless
ppmv	Parts per million by volume
Q_{SL}	Annual solar heat exchanged with sea water, J yr^{-1}
Q_E	Annual latent heat removed by surface evaporation, J yr^{-1}
Q_{IN}	Earth's internal heat, J yr^{-1}
T_S	Average sea surface temperature, °C.
T_{S0}	Initial average sea surface temperature, °C.
T	Temperature of the deep sea water of the southern oceans, °C.
T_N	Sea temperature of the northern oceans, about equal to T_O, °C
T_O	Average temperature of the deep ocean, °C
T_{db}	Terrestrial air dry bulb temperature, °K
T_{wb}	Terrestrial air wet bulb temperature, °K
t	Time, in years
yr	Abbreviation of year